



## Study and optimisation of manganese oxide-based electrodes for electrochemical supercapacitors

P. Staiti\*, F. Lufrano

CNR-ITAE, Istituto di Tecnologie Avanzate per l'Energia "Nicola Giordano", Via Salita S. Lucia n. 5, 98126 S. Lucia, Messina, Italy

### ARTICLE INFO

#### Article history:

Received 29 May 2008

Received in revised form 25 August 2008

Accepted 19 October 2008

Available online 5 November 2008

#### Keywords:

Manganese oxide  
Pseudo-capacitance  
Supercapacitor

### ABSTRACT

A manganese oxide material was synthesised by an easy precipitation method based on reduction of potassium permanganate(VII) with a manganese(II) salt. The material was treated at different temperatures to study the effect of thermal treatment on capacitive property. The best capacitive performance was obtained with the material treated at 200 °C. This material was used to prepare electrodes with different amounts of polymer binder, carbon black and graphite fibres to individuate the optimal composition that gave the best electrochemical performances. It was found that graphite fibres improve the electrochemical performance of electrodes. The highest specific capacitance ( $267 \text{ F g}^{-1} \text{ MnO}_x$ ) was obtained with an electrode containing 70% of  $\text{MnO}_x$ , 15% of carbon black, 10% of graphite fibres and 5% of PVDF. This electrode, with CB/GF ratio of 1.5, showed a higher utilization of manganese oxide. The results reported in the present paper further confirmed that manganese oxide is a very interesting material for supercapacitor application.

© 2008 Elsevier B.V. All rights reserved.

### 1. Introduction

Metal oxides with various valence states are acquiring growing interest in the preparation of electrodes with pseudocapacitive properties for supercapacitor applications. Ruthenium oxide is among these materials that showing the best pseudocapacitive properties [1–3], nevertheless the high cost, the limited availability and the polluting effect on environment make this not attractive for large scale use. Thus, actually other metal oxides such as iridium oxide, cobalt oxide, nickel oxide, vanadium oxide, bismuth oxide, molybdenum oxide, tin oxide, manganese oxide, etc. are investigated as possible substitute [4–12]. Manganese oxide is a material very attractive for its high availability, low cost and no-polluting effects compared to ruthenium oxide. For these reasons, nowadays this material is deeply studied in order to attain more knowledge about its intrinsic properties and to find relations between morphological, structural, compositional characteristics of the material with the electrochemical performance of supercapacitor based on this material [12–34]. A great number of papers is present in current literature reporting results obtained from manganese oxides prepared by various methods to form materials of different atomic composition, structure and morphology. In fact, manganese oxide materials were prepared by methods, such as chemical synthesis

[13,14], sol–gel synthesis [15–18], hydrothermal synthesis [19–22], electrochemical deposition [23–29], electrostatic spray deposition [30,31], physical vapour deposition [32–34], etc., to which in most cases thermal and/or electrochemical treatments followed to modify the composition, the morphology and the structure of the raw materials. An analysis of the best results in terms of specific capacitance referred to manganese oxides obtained by the different preparation methods will be hereafter reported.

Prasad and Miura [24] prepared manganese oxide by potentiodynamic deposition on a stainless steel substrate and obtained specific capacitance (SC) of  $480 \text{ F g}^{-1}$  at scan rate of  $10 \text{ mV s}^{-1}$ . The authors investigated electrode films with very low material loadings, between 0.1 and  $0.23 \text{ mg cm}^{-2}$ . Broughton and Brett [32] reported results of SC of  $700 \text{ F g}^{-1}$  obtained from  $\text{MnO}_2$  films prepared by anodic oxidation of sputtered manganese films of  $25\text{--}75 \text{ } \mu\text{g cm}^{-2}$  and Pang et al. [15] SC of  $698 \text{ F g}^{-1}$  from  $\text{MnO}_2$  films obtained by sol–gel synthesis with subsequent annealing at 300 °C. These latter authors showed that the SC reduced at about half when the mass of electrode was varied from 1 to  $13 \text{ } \mu\text{g cm}^{-2}$ . Toupin et al. [14] reported interesting results from manganese oxide synthesised by a easy method based on chemical reaction of potassium permanganate with manganese sulphate in aqueous solution. They reported SC of  $180 \text{ F g}^{-1}$  from the untreated powder and, a little different value of  $160 \text{ F g}^{-1}$  from the powder heated for 3 h between 100 and 200 °C, that was a 12% lower of the initial value. The sample treated at 600 °C for 3 h induced a capacitance of only  $40 \text{ F g}^{-1}$ , that represented only 22% of the initial SC. Their conclu-

\* Corresponding author. Tel.: +39 090 624226; fax: +39 090 624247.  
E-mail address: [staiti@itae.cnr.it](mailto:staiti@itae.cnr.it) (P. Staiti).

sions were that the pseudocapacitive phenomenon occurred in a very limited thickness of manganese oxide and thus the specific capacitance was limited by the available surface area of the material. For these authors the thermal treatment at 100–200 °C of the untreated material produced a small increase of the capacitance due to the loss of water molecules but also a greater decrease of capacitance due to the decrease of surface area, with the second effect predominant and producing a lowering of capacitive performance. No information was given by the authors on the manganese oxide loadings of electrodes.

The present paper provides new insights into the mechanism of capacitive improvement of manganese oxide-based electrodes by varying the amounts of additive materials, i.e. carbon powder, graphite fibres and binding polymer. Moreover, electrodes with manganese oxide loadings available for practical applications (about 10 mg of  $\text{MnO}_x \text{ cm}^{-2}$ ) are investigated. The oxide is prepared by the co-precipitation method following the procedure reported by Toupin et al. [14], consisting essentially in the reaction of a permanganate salt with a manganese(II) salt. A study on thermal treatment of the manganese oxide is also made to individuate the temperature at which the highest capacitive performance of the material are achieved. The prepared manganese oxide samples are analysed for the morphological, structural and surface characteristics by SEM, XRD and BET analyses. In a second phase, the best performing material is used for the preparation of electrodes of different composition to evaluate the influence of the addition of different amounts of fillers on electrochemical performances. In particular, a study of the influence of different amounts of activated carbon, graphite fibres and polymer binder on the electrochemical performances of the electrodes is carried out. The obtained results permit to individuate (a) the composition that gives the best capacitive performance, and (b) the content of carbon black and graphite fibres that allow to maximize the utilization of manganese oxide and minimize the internal resistance of the electrodes.

## 2. Experimental

### 2.1. Preparation of the manganese oxide materials

Manganese oxide was synthesised by precipitation from an aqueous solution of potassium permanganate(VII) and manganese(II) chloride, at 25 °C. More specifically, a 100 ml solution containing 0.03 moles of  $\text{MnCl}_2$  was added drop by drop during 30 min under continuous stirring to a 200 ml solution containing 0.02 moles of  $\text{KMnO}_4$ . The so-obtained suspension was stirred for 6 h during which a dark-brown precipitate was formed. After stopping the stirring and decanting for 16 h the suspension two distinct phases were formed consisting of a fine precipitate and a supernatant liquor. The liquor was removed by the use of a pipette and

the precipitate was washed several times with distilled water in the beaker before filtering under vacuum. The formed precipitate was finally dried at 70 °C for 16 h after which a fine powder of manganese oxide was obtained.

The  $\text{MnO}_x$  powder was divided in three portions, the first one remained as-obtained after drying, the second and the third were thermally treated at 200 and at 400 °C, respectively. The as-obtained, the thermal treated at 200 °C and the thermal treated at 400 °C materials will be named in the paper MN70, MN200 and MN400, respectively.

### 2.2. Preparation of the electrodes

Electrodes were prepared by a casting technique by spreading the inks, containing the manganese oxide material, the PVDF binder, the carbon black powder, the solvent and in some cases the graphite fibres, which were thoroughly mixed in a mortar, on a 1.5  $\text{cm}^2$  titanium net disk. The metallic disk used as support of the capacitive layer limited the contact resistance of the electrode inserted in the test cell. Carbon powder and graphite fibres were added to the inks to improve electric conductivity and mechanical stability of the electrodes and to increase the dispersion of manganese oxide. The prepared electrodes differed for the manganese oxide material (MN70, MN200 and MN400), and/or for the amount of carbon powder and graphite fibres, and/or for the amounts of polymer binder.

Polyvinylidene fluoride (PVDF) was a product Aldrich in grain form that before its use in the ink formation was dissolved in *N,N*-dimethylacetamide. Shawinigan Acetylene Black furnished by Chevron Phillips with purity >99.9% and surface area of 75  $\text{m}^2 \text{ g}^{-1}$  was the carbon black used in the electrodes. Graphite fibres of length 100–200  $\mu\text{m}$  were prepared in-house by milling for 3 min in a high speed grinder a carbon fabric Avcarb 1071 furnished by Ballard Material Products, Inc. (MA, USA).

All the electrodes were prepared with  $\text{MnO}_x$  amounts suitable for practical application in supercapacitors, specifically they contained  $6.5 \pm 0.1 \text{ mg MnO}_x \text{ cm}^{-2}$ . The compositions of all the electrodes investigated in the present work are reported in Table 1. A first set of three electrodes was prepared to study the effect of thermal treatment on the capacitive performance of manganese oxide (electrodes MN70-AB1, MN200-AB2, MN400-AB3), and a second set, to study the influence of the carbon black/graphite fibres ratio and of the binding agent content on the electrochemical performance of manganese oxide (MN200-ABG1/MN200-ABG7).

### 2.3. Characterization of materials and electrodes

A scanning electron microscopy Philips XL Series equipped with EDX module model New XL-30, an X-ray diffractometer Philips

**Table 1**

List of investigated electrodes with compositions, specific capacitances, variation rates of SC and resistances.

Electrode	$\text{MnO}_x$ (%)	Acetylene black (%)	Graphite fibres (%)	PVDF (%)	AB/GF ratio	Specific capacitance at 2 $\text{mA cm}^{-2}$ <sup>a</sup> ( $\text{F g}^{-1}$ )	Specific capacitance at 20 $\text{mA cm}^{-2}$ <sup>a</sup> ( $\text{F g}^{-1}$ )	Decreasing rate of SC from 2 to 20 $\text{mA cm}^{-2}$	Resistance <sup>b</sup> ( $\Omega \text{ cm}^2$ )
MN70-AB1	70	20	0	10	–	247	73	70.4%	14.2
MN200-AB2	70	20	0	10	–	241	115	52.3%	6.6
MN400-AB3	70	20	0	10	–	211	77	63.5%	9.3
MN200-ABG1	70	5	15	10	0.33	230	111	51.7%	10.5
MN200-ABG2	70	10	10	10	1	244	123	49.5%	5.4
MN200-ABG3	70	10	15	5	0.66	253	151	40.3%	4.5
MN200-ABG4	70	12.5	12.5	5	1	246	178	27.6%	2.6
MN200-ABG5	70	15	10	5	1.5	267	193	27.7%	3.9
MN200-ABG6	70	16.6	8.3	5	2	230	157	31.7%	3.1
MN200-ABG7	70	17.5	7.5	5	2.33	245	129	47.3%	3.0

<sup>a</sup> Values calculated from discharge branches of galvanostatic charge/discharge tests.

<sup>b</sup> Resistances calculated from potential drops at 0.8 V after current inversion; current inversion from +5 to –5  $\text{mA cm}^{-2}$ .

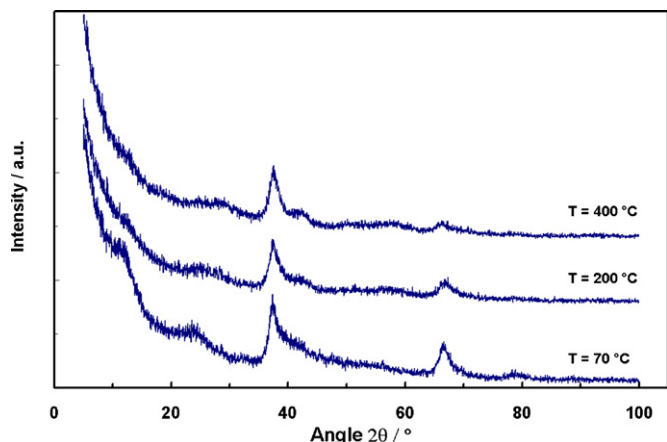


Fig. 1. XRD patterns of  $\text{MnO}_x$  materials treated at different temperatures.

X'Pert equipped with  $\text{Cu K}\alpha$  source, and a Sorptomatic 1990 ThermoQuest apparatus, were used to analyse the morphological, structural and surface characteristics of the manganese oxide.

Electrochemical characterization of electrodes was carried out in a three-electrode cell connected to an Amel equipment for the galvanostatic and potentiodynamic tests. Galvanostatic charge/discharge (CD) and cyclic voltammetry (CV) tests were carried out in a cell provided of a working electrode, where the tested electrode was fixed, and of a platinum disk and a saturated calomel electrode (SCE) as counter and reference electrodes, respectively. A 0.1 M  $\text{Na}_2\text{SO}_4$  solution was used as electrolyte. The exposed area of tested electrodes was  $1 \text{ cm}^2$ . CD and CV tests were conducted at current densities of 2, 5, 10,  $20 \text{ mA cm}^{-2}$  and at voltage sweep rates of 2, 5, 10,  $20 \text{ mV s}^{-1}$ , respectively, by cycling the potential of the working electrode between  $-0.2$  and  $+0.8 \text{ V}$  with respect to SCE. The results of CD and CV tests were collected after an initial stabilising time carried out cycling the electrodes in CV mode at  $10 \text{ mV s}^{-1}$  for 50 cycles. In fact, it was found that during the first 10–20 cyclic voltammograms some variation on the shape of curves can be evidenced, but after 50 cycles the voltammograms were reproducible.

### 3. Results and discussion

#### 3.1. Structural and morphological properties

Fig. 1 shows XRD patterns of as-synthesised and of thermal treated at 200 and  $400^\circ\text{C}$  manganese oxide materials. The XRD analysis reveals similar structural characteristics for the different thermally treated samples, which show evident broad peaks at  $2\theta = 37.5$  and  $67.0^\circ$ . Other less pronounced broad peaks are at  $11.5$ ,  $24$ – $29$ ,  $42.6^\circ$ . These peaks are attributable to the  $\alpha\text{-MnO}_2$  phase in agreement with similar XRD patterns reported in literature [35,36]. The micro-morphological aspect of the materials is depicted by SEM images of Fig. 2. The figure shows that spherical grains of average dimension of about  $300 \text{ nm}$  appear linked to form bigger agglomerates. This situation is observed for all the different thermally treated samples. The grain particles of the MN70 (Fig. 2a and b) and MN200 (Fig. 2c and d) samples appear formed by small plate-like particles stuck each to the other while the grain particles of the MN400 sample (Fig. 2 e and f) appear formed by petal-like particles which extend out the grains. The BET surface area of the sample treated at  $70^\circ\text{C}$  is  $6 \text{ m}^2 \text{ g}^{-1}$  while that obtained from the sample treated at  $200^\circ\text{C}$ , that appears similar by SEM analysis to the former, is  $36 \text{ m}^2 \text{ g}^{-1}$ . Furthermore, the sample treated at  $400^\circ\text{C}$ , that appears by SEM analysis morphologically different from that treated at  $200^\circ\text{C}$ , has a similar S.A. of  $37 \text{ m}^2 \text{ g}^{-1}$ . Thus, a great difference of

S.A. was found between the MN70 and MN200 samples, while similar values of S.A. were found for the MN200 and MN400 samples. It is possible that the very low surface area of MN70 sample is caused from the water still impregnated in the porous structure after the degassing treatment carried out before the BET analysis under vacuum at the temperature of  $70^\circ\text{C}$  for 3 h. The degassing treatment cannot be made at higher temperature to avoid morphological and structural modifications of the material. The other two materials, MN200 and MN400, are degassed at a higher temperature of  $150^\circ\text{C}$ .

EDX analyses were also performed on the three samples to determinate the potassium contents. Five analyses were made on different regions of each sample to have representative values. The results of analyses obtained from each sample were very similar and they were also similar to those obtained from the analyses of the other samples. Thus an atomic ratio  $\text{K/Mn}$  of  $0.038 \pm 0.004$  is considered representative for all the  $\text{MnO}_x$  samples. A typical EDX spectrum is reported in Fig. 3.

#### 3.2. Electrochemical properties

Three electrodes (MN70-AB1, MN200-AB2, MN400-AB3) were prepared with the different treated manganese oxide materials (see Table 1) and analysed for the electrochemical performances by CV and galvanostatic CD tests. The amounts of charge, which were obtained from the discharge process during the galvanostatic charge/discharge tests were used to calculate the SC of the material using the following formula:

$$\text{SC} = \frac{I \cdot \Delta t}{\Delta V \cdot q}$$

In which  $I$  and  $\Delta t$  of numerator are the current and the discharge time, respectively, and  $\Delta V$  and  $q$  of denominator the potential difference and the weight of the manganese oxide contained in the electrode, respectively. Preliminary tests carried out on two electrodes, one with only carbon black and the other one with carbon black and graphite fibres, gave specific capacitance for these materials very low and thus their contributes to the overall capacitance in the electrodes with manganese oxide can be negligible without appreciable error.

Fig. 4 reports data of SCs obtained from galvanostatic tests performed at current densities of 2, 5, 10,  $20 \text{ mA cm}^{-2}$  for the three above mentioned electrodes. The best results of specific capacitance were obtained from the electrode with manganese oxide treated at  $200^\circ\text{C}$  (MN200-AB2); only the test conducted at  $\pm 2 \text{ mA cm}^{-2}$  gave a better result with the electrode treated at  $70^\circ\text{C}$  (MN70-AB1). Fig. 5 reports cyclic voltammetry curves recorded during tests carried out at the voltage sweep rate of  $10 \text{ mV s}^{-1}$  for the three samples and, Fig. 6 the charge–discharge curves recorded during the tests performed at the constant current density of  $\pm 5 \text{ mA cm}^{-2}$  for the same electrodes. Also from the data collected from CV tests, represented in Fig. 5, it was evident that the best capacitive performance in the reported conditions was obtained by the MN200-AB2 electrode. Figs. 5 and 6 show also that the electrode with manganese oxide treated at the lowest temperature presents the highest internal resistance. This qualitative difference among the electrodes can be observed in the cyclic voltammetry through the slower variation of current sign after the inversion of voltage sweep and in the galvanostatic charge–discharge tests from the jump and drop of potential after inversion of sign of current at the minimum and maximum potential. The main reason of the lower performance found with the electrode treated at  $70^\circ\text{C}$  is probably due to its high electric resistance while that of electrode treated at  $400^\circ\text{C}$  to its poorer pseudocapacitive property. The fact that the main contribution to the capacitance in these electrodes derives from pseudocapacitance is demonstrated taking into



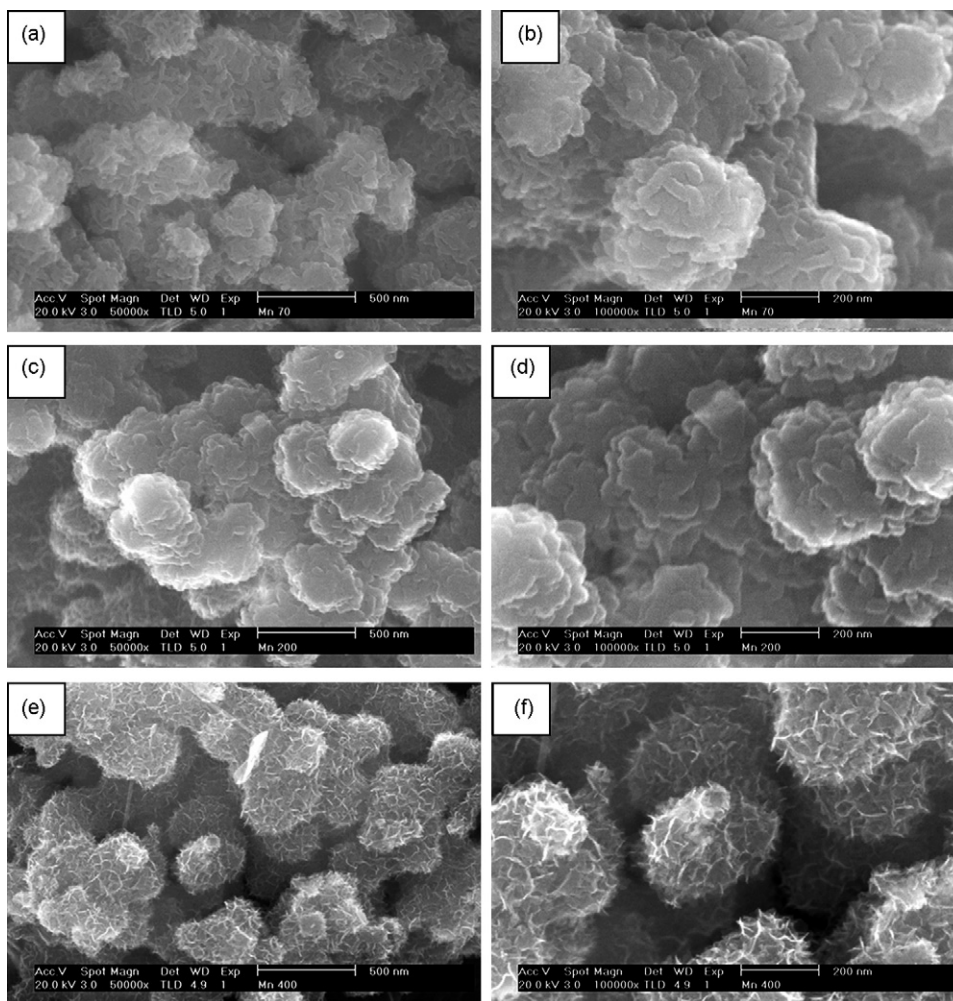


Fig. 2. SEM images at different magnifications of MN70 (a) and (b), MN200 (c) and (d), and MN400 (e) and (f).

account the same considerations made from Toupin et al. [14]. In fact, if the capacitance is due to the double layer formation, it should depend from the surface area of the material. At the maximum measured surface area of  $37 \text{ m}^2 \text{ g}^{-1}$ , and considering an average value of capacitance of  $20 \mu\text{F cm}^{-2}$  [14], a maximum value of  $7.4 \text{ F g}^{-1} \text{ MnO}_x$  could be obtained, that is a value very much lower than those effectively found in this work for this material (about  $250 \text{ F g}^{-1}$ ). Another interesting aspect observed in the graphic of CD tests reported in

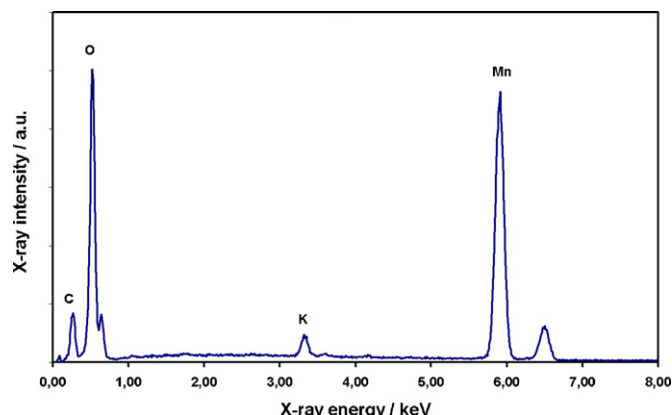
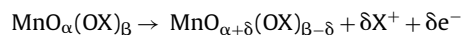


Fig. 3. Typical EDX spectrum of synthesised manganese oxide.

Fig. 6 is that the electric resistance at the beginning of the charging process is higher than that at the beginning of the discharging process, as evidenced by the jumps of potential at  $-0.2 \text{ V}$  and drops of potential at  $0.8 \text{ V}$ , respectively. The explanation of this effect could be that during the charging process, free protons and/or cations form at the interface electrode/electrolyte and these increase the ionic conductivity of the solution or that a more conductive phase of manganese oxide is formed. The first hypothesis is more acceptable while it is less probable that the metal with a higher oxidation state, that forms during charging to  $0.8 \text{ V}$ , is more conductive. In any case, this effect merits to be more deeply studied and this will be a topic of our future work. The electrochemical oxidation process occurring at the positive electrode during the charging step is the following.



The formation of free protonic or cationic species ( $\text{X}^+$ ) which increase the ionic conductivity of the electrolyte could also be the reason of the continuous increase of current during cyclic voltammetry charging of the electrodes (Fig. 5). The electrode MN200-AB2, that shows the best capacitive performance for the manganese oxide, presents internal resistance of about  $6.6 \Omega \text{ cm}^2$  (esteemed by the voltage drop measured after inversion of current at  $0.8 \text{ V}$ ). This value if would be lowered could produce further improvement of the capacitive performance of this material. For this reason, a series of electrodes based on MN200 material was prepared by adding various amounts of carbon black, graphite binder and polymer binder.

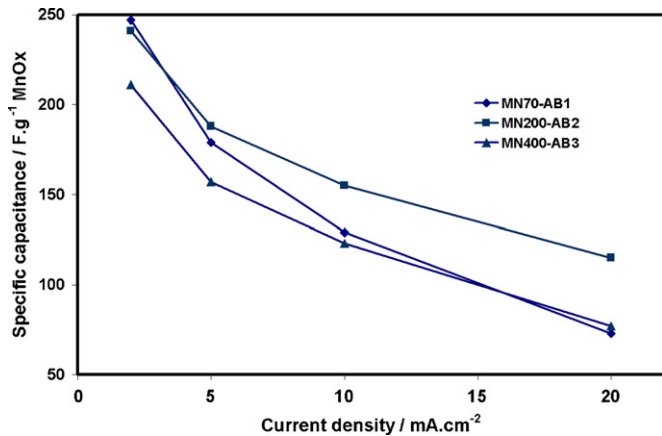


Fig. 4. Specific capacitance in function of current density obtained from electrodes prepared with different treated manganese oxides.

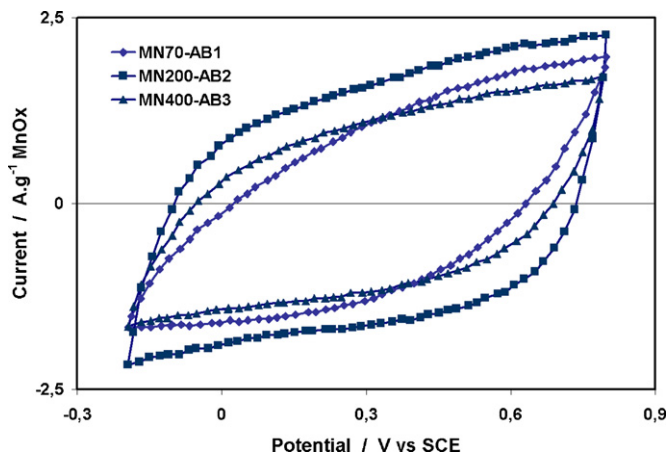


Fig. 5. Cyclic voltammograms of the electrodes prepared with different treated manganese oxides. Scanning rate = 10 mV s<sup>-1</sup>.

The list of these electrodes with the respective compositions, specific capacitances, rates of SC decreasing and internal resistances are reported in Table 1 (series from MN200-ABG1 to MN200-ABG7). Fig. 7 reports results of specific capacitance obtained at various discharge currents from electrodes with graphite fibres (MN200-ABG1 and MN200-ABG2) and without graphite fibres (MN200-AB2). In the same figure the specific capacitance of an electrode MN200-ABG4 with the same ratio between carbon black and graphite

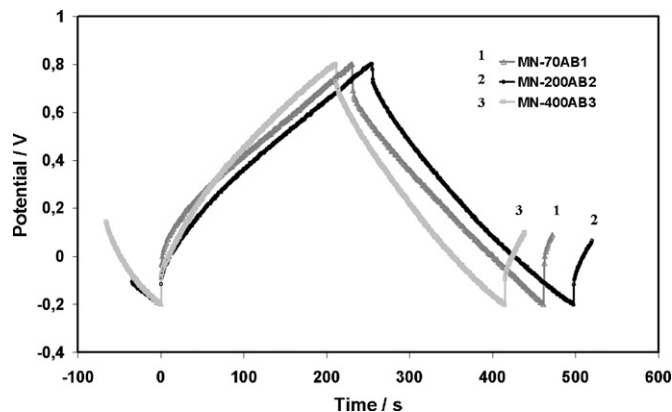


Fig. 6. Curves of charge/discharge test obtained from electrodes prepared with different treated manganese oxides. Current density =  $\pm 5$  mA cm<sup>-2</sup>.

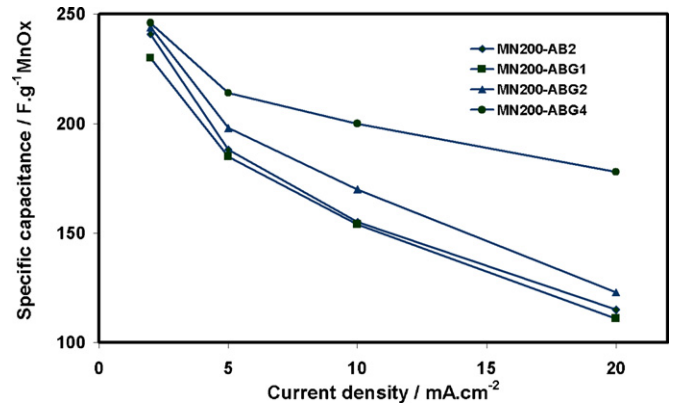


Fig. 7. Specific capacitance versus current density of the electrodes prepared with MnO<sub>x</sub> treated at 200 °C, 10% of PVDF and carbon black (MN200-AB2) or with carbon black and graphite fibres (MN200-ABG1, MN200-ABG2). The ratio CB/GF is 0.33 in MN200-ABG1 and 1 in MN200-ABG2. The MN200-ABG4 electrode contains 5% of PVDF and has CB/GF ratio = 1.

fibres of the MN200-ABG2 electrode (CB/GF = 1) but with a lower amount of polymer binder is also reported. The figure evidences the importance of the presence of graphite fibres in the electrode, that improves the capacitive performance of manganese oxide, but also the necessity to identify the more appropriate CB/GF ratio to maximize the capacitive performance. In fact, the results obtained by the MN200-ABG1 electrode with a lower CB/GF ratio than MN200-ABG2 electrode appeared very similar to those obtained with MN200-AB2 that does not contain graphite fibres. It is probably that the presence of graphite fibres with an insufficient amount of carbon powder forms an electrode not well packed with a large void fraction that increases the internal resistance as it is evidenced in Table 1 (electrode MN200-ABG1). A deeper study of the effect of the CB/GF ratio in the electrode has been done with the electrodes containing a lower loading of polymer binder (5 wt.% of PVDF in the electrode) after the observation that the results obtained from MN200-ABG4 electrode, also represented in Fig. 6, prepared with the same CB/GF ratio of MN200-ABG2 electrode but with a lower PVDF content, gave very much higher capacitive performance. Thus, the addition of graphite fibres in the electrode has a positive effect on the specific capacitance and this is evidenced in the figure from the comparison of the results obtained by the electrode MN1-200AB2 with those of the electrode MN-200 ABG2 containing the same amount of polymer binder (10%). Another important advantage deriving from the use of graphite fibres is that a lower amount of polymer binder may be used without decreasing the mechanical stability of electrodes. The lowering of the polymer binder in the composition of electrodes produces as an effect the increase of SC of MnO<sub>x</sub> especially at the higher current densities as it is evidenced in Fig. 7 and Table 1 from the comparison of the results attained from the electrode MN1-200ABG2 (with 10% of PVDF) with those of the electrode MN1-200ABG4 (with 5% of PVDF) and both having CB/GF ratio = 1. Thus, a series of electrodes, from MN200-ABG3 to MN200-ABG7, were prepared with 5% of PVDF and various percentages of carbon black and graphite fibres to investigate the effect of electrode composition on the electrode performances. To have a clearer representation of the changes of the electrode performance with the CB/GF ratio, the specific capacitances obtained from CD tests were reported in Fig. 8 as a function of the CB/GF ratio. The figures evidence that at all the investigated current densities (2, 5, 10, 20 mA cm<sup>-2</sup>) the electrode with CB/GF ratio 1.5 gives the best SCs and, the improvements of the performance are more pronounced at the higher current densities where the effects of the lower internal resistance become more evident. At the lowest

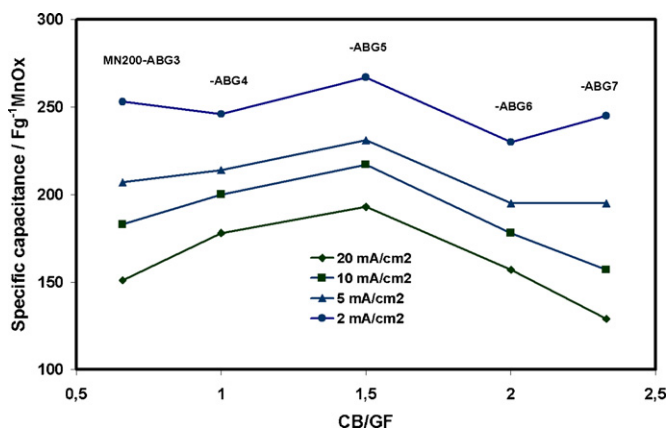


Fig. 8. Specific capacitance versus CB/GF ratio of the electrodes prepared with  $\text{MnO}_x$  treated at  $200^\circ\text{C}$  and having 5% of PVDF obtained at different current densities.

value of the investigated current densities ( $2\text{ mA cm}^{-2}$ ) there is not a clear trend of capacitance with the CB/GF ratio, because the ohmic losses in this condition become negligible and other effects could prevail. At the highest investigated CB/GF ratio (2.33) the behaviour of electrode is very similar to that of the electrode containing only carbon black (without graphite) as it is observed comparing the results of MN200-AB2 electrode of Fig. 7 with the MN200-ABG7 electrode of Fig. 8. Analysing all the results reported in this paper, we may affirm that the best result of specific capacitance,  $267\text{ Fg}^{-1}$  of  $\text{MnO}_x$ , is obtained with the manganese oxide treated at  $200^\circ\text{C}$  with the electrode (MN200-ABG5) having 5 wt.% of binder content and an acetylene black/graphite fibres ratio of 1.5. The minimum electrode resistance is obtained with the electrode MN200-ABG4 that has CB/GF = 1. Thus, we may affirm that the CB/GF ratio = 1 is optimal to obtain the minimum resistance and the CB/GF ratio = 1.5 is optimal to have a higher utilization of  $\text{MnO}_x$ . These two electrodes also present a lower variation of specific capacitance when they are tested at 2 and at  $20\text{ mA cm}^{-2}$ , that is due to their better internal structure for ion mobility. The calculated energy density and power density for the electrode MN200-ABG5 are  $37\text{ Wh kg}^{-1}$  of  $\text{MnO}_x$  and  $9.8\text{ kW kg}^{-1}$  of  $\text{MnO}_x$ , respectively.

#### 4. Conclusions

A manganese oxide material was synthesised by an easy precipitation method, involving an oxidant manganese salt (potassium permanganate) and a reducing manganese salt (manganese chloride), and a subsequent heat treatment. The materials treated at  $200^\circ\text{C}$  for 3 h showed the best capacitive performance. A mixed oxide is formed having general formula  $\text{MnO}_x(\text{OX})_y$  with X proton or potassium ion. An electrode prepared with manganese oxide treated at  $200^\circ\text{C}$  and optimised for the polymer binder content and carbon black/graphite fibres ratio gave specific capacitance

of  $267\text{ Fg}^{-1}$  and energy density and power density of 37 and  $9.8\text{ kW kg}^{-1}$ , respectively. This electrode was prepared with 6.5 mg of  $\text{MnO}_x\text{ cm}^{-2}$ , 5% of PVDF and 1.5 CB/GF ratio. It evidenced also the lower decreasing rate of specific capacitance by galvanostatic tests performed at 2 and  $20\text{ mA cm}^{-2}$ . The electrode with CB/GF ratio = 1.5 presented the higher utilization of  $\text{MnO}_x$ . This results, taking into account the relatively high content of manganese oxide in the electrode respect to those commonly reported in literature, are very interesting in the perspective of practical application of manganese oxide in supercapacitors.

#### References

- [1] B.E. Conway, *Electrochemical Supercapacitors, Scientific Fundamental and Technological Applications*, Kluwer Academic/Plenum Press, New York, 1999, pp. 259–297.
- [2] J.P. Zheng, J. Huang, T.R. Jow, *J. Electrochem. Soc.* 144 (1997) 2026–2031.
- [3] J.P. Zheng, T.R. Jow, *Electrochem. Solid State Lett.* 2 (1999) 359–361.
- [4] A.A.F. Grupioni, E. Arashiro, T.A.F. Lassali, *Electrochim. Acta* 48 (2002) 407–418.
- [5] C. Lin, J.A. Ritter, B.N. Popov, *J. Electrochem. Soc.* 145 (1998) 4097–4103.
- [6] V. Srinivasan, J.W. Weidner, *J. Power Sources* 108 (2002) 15–20.
- [7] V. Srinivasan, J.W. Weidner, *J. Electrochem. Soc.* 147 (2000) 880–885.
- [8] K.R. Prasad, N. Miura, *Electrochem. Commun.* 6 (2004) 849–852.
- [9] Z.J. Lao, K. Konstantinov, Y. Tournaire, S.H. Ng, G.X. Wang, H.K. Liu, *J. Power Sources* 162 (2006) 1451–1454.
- [10] P.P. Gujar, V.R. Shinde, C.D. Lokhande, S.-H. Han, *J. Power Sources* 161 (2006) 1479–1485.
- [11] W. Sugimoto, T. Ohnuma, Y. Murakami, Y. Takasu, *Electrochem. Solid State Lett.* 4 (2001) A145–A147.
- [12] H.Y. Lee, J.B. Goodenough, *J. Solid State Chem.* 144 (1999) 220–223.
- [13] X. Wang, Y. Li, *Chem. Commun.* (2002) 764–765.
- [14] M. Toupin, T. Brousse, D. Belanger, *Chem. Mater.* 14 (2002) 3946–3952.
- [15] S.C. Pang, M.A. Anderson, T.W. Chapman, *J. Electrochem. Soc.* 147 (2000) 444–450.
- [16] S.F. Chin, S.C. Pang, M.A. Anderson, *J. Electrochem. Soc.* 149 (2002) A379–A384.
- [17] R.N. Reddy, R.G. Reddy, *J. Power Sources* 124 (2003) 330–337.
- [18] C.-K. Lin, K.-H. Chuang, C.-Y. Lin, C.-Y. Tsay, C.-Y. Chen, *Surf. Coat. Technol.* 202 (2007) 1272–1276.
- [19] R. Chen, T. Chirayil, P. Zavalij, M.S. Whittingham, *Solid State Ionics* 86–88 (1996) 1–7.
- [20] R. Chen, M.S. Whittingham, *J. Electrochem. Soc.* 144 (1997) L64–L67.
- [21] M. Tabuchi, K. Ado, H. Kobayashi, H. Kageyama, C. Masquelier, A. Kondo, R. Kanno, *J. Electrochem. Soc.* 145 (1998) L49–L52.
- [22] V. Subramanian, H.W. Zhu, R. Vajtai, P.M. Ajayan, B.Q. Wei, *J. Phys. Chem. B* 109 (2005) 20207–20214.
- [23] J.-K. Chang, W.-T. Tsai, *J. Electrochem. Soc.* 150 (2003) A1333–A1338.
- [24] K.R. Prasad, N. Miura, *J. Power Sources* 135 (2004) 354–360.
- [25] M. Nakayama, A. Tanaka, Y. Sato, T. Tonosaki, K. Ogura, *Langmuir* 21 (2005) 5907–5913.
- [26] N. Nagarajan, H. Humadi, I. Zhitomirsky, *Electrochim. Acta* 51 (2006) 3039–3045.
- [27] T. Xue, C.-L. Xu, D.-D. Zhao, X.-H. Li, H.-L. Li, *J. Power Sources* 164 (2007) 953–958.
- [28] M. Nakayama, T. Kanaya, R. Inoue, *Electrochem. Commun.* 9 (2007) 1154–1158.
- [29] J.N. Broughton, M.J. Brett, *Electrochim. Acta* 50 (2005) 4814–4819.
- [30] Y. Dai, K. Wang, J. Zhao, J. Xie, *J. Power Sources* 161 (2006) 737–742.
- [31] K.-W. Nam, K.-B. Kim, *J. Electrochem. Soc.* 153 (2006) A81–A88.
- [32] J.N. Broughton, M.J. Brett, *Electrochim. Acta* 49 (2004) 4439–4446.
- [33] B. Djurfors, J.N. Broughton, M.J. Brett, D.G. Ivey, *J. Power Sources* 156 (2006) 741–747.
- [34] B. Djurfors, J.N. Broughton, M.J. Brett, D.G. Ivey, *J. Electrochem. Soc.* 153 (2006) A64–A68.
- [35] C. Xu, B. Li, H. Du, F. Kang, Y. Zeng, *J. Power Sources* 180 (2008) 664–670.
- [36] M. Xu, L. Kong, W. Zhou, H. Li, *J. Phys. Chem. C* 111 (2007) 19141–19147.